

## Assessment of remote sensing empirical algorithms to retrieve colored dissolved organic matter in the Lower Amazon River

Aline de Matos Valerio<sup>1</sup>  
Milton Kampel<sup>1</sup>  
Vincent Vantrepotte<sup>2</sup>  
Nicholas D. Ward<sup>3</sup>  
Henrique O. Sawakuchi<sup>4</sup>  
Diani Fernanda da Silva Less<sup>5</sup>  
Joel Diniz<sup>5</sup>  
Vania Neu<sup>6</sup>  
Alan C. Cunha<sup>5</sup>  
Alex V. Krusche<sup>4</sup>  
Jeffrey E. Richey<sup>7</sup>

<sup>1</sup>Instituto Nacional de Pesquisas Espaciais - INPE  
Caixa Postal 515 - 12227-010 - São José dos Campos - SP, Brasil  
{alineval, milton}@dsr.inpe.br

<sup>2</sup>Centre National de la Recherche Scientifique - CNRS  
USR3456, 97334 Cayenne, French Guiana  
vincent.vantrepotte@univ-littoral.fr

<sup>3</sup>University of Florida - UF  
St. Augustine, FL, United States of America  
nickdward@gmail.com

<sup>4</sup>Universidade de São Paulo - USP/CENA  
Caixa Postal 96 - 13416-000 - Piracicaba - SP, Brasil  
riqueoliveira@yahoo.com.br  
alex@cena.usp.br

<sup>5</sup>Universidade Federal do Amapá – UNIFAP  
Caixa Postal 261 – 68906-970 - Macapá - AP, Brasil  
diani.engambiental@gmail.com  
jemdiniz@yahoo.com.br  
alancunha12@gmail.com

<sup>6</sup>Universidade Federal Rural da Amazônia – UFRA  
Caixa Postal 917 - 66077-530 – Belém - PA, Brasil  
vania.neu@ufra.edu.br

<sup>7</sup>University of Washington – UW  
98195, Seattle - UW, United States of America  
jrichey@uw.edu

**Abstract.** There are many empirical algorithms described in the literature to estimate colored dissolved organic matter (CDOM) by remote sensing. When the measurements are acquired in turbid water, new algorithms might be required to better characterize regional optical characteristics. The aim of this study is the assessment of current empirical algorithms to retrieve CDOM absorption coefficient ( $a_{\text{cdom}}$ ) by remote sensing in the Lower Amazon. This is a region where very turbid waters mix with clear water from tributary rivers. Surface water

samples were collected concurrent with radiometric measurements in different stations along the study area, throughout the annual hydrological cycle: Rising, High, Falling and Low water. Remote sensing reflectance ( $R_{rs}$ ) was estimated from in situ radiometric data presenting a low coefficient of variation in the range of 400-840 nm. Six empirical algorithms were used to estimate  $a_{cdom}$  (G11, K05, B05, M14, T11 and K15) from  $R_{rs}$  showing high values even in the green spectrum. The K15 ( $R^2=0.57$ ; RMSE = 0.09; p-value<0.05) showed the best performance when compared to all *in situ*  $a_{cdom}$  measurements. However, when the dataset is partitioned into clear water rivers and Amazon River the results are different. For clear water the algorithms presented a better performance (e.g. K15  $R^2=0.68$ ; RMSE = 0.14, p-value<0.05), and no significant correlation was obtained for the Amazon River. The results suggest that other optically active constituents are interfering in the retrieve of CDOM, and it is likely to be suspended sediments. Therefore, different methodological approaches should be explored to correct for this interference.

**Keywords:** CDOM, turbid water, bio-optical properties, matéria orgânica dissolvida colorida, águas túrbidas, propriedades bio-ópticas.

## 1. Introduction

Colored dissolved organic matter (CDOM) is a fraction of the dissolved organic matter (DOM) that absorbs ultraviolet (UV) and visible light, hence has an important role in the optical properties of aquatic systems. In freshwaters, CDOM is usually allochthonous and influenced by land surface processes (Wetzel and Likens, 2000). Many empirical CDOM algorithms have been developed in the last decades and these algorithms are sensitive to changes in the specific composition of water constituents (Zhu et al., 2014). The first empirical algorithm developed to retrieve CDOM used the blue-green ratio, more suitable for waters with low CDOM as well as low suspended particles (i.e. oceanic waters) (Tassan, 1994). With the increase of CDOM towards continental shelf, estuarine and inland waters, new algorithms were developed using different band ratios (Brezonik et al., 2005; Kutser et al., 2005; Griffin et al., 2011; Tiwari and Shanmugam, 2011; Mannino et al., 2014; Kutser et al., 2015). While numerous studies have focused on the estimation of CDOM using ocean color remote sensing for coastal waters applications, efforts must be performed to better understand the link between water's apparent and inherent optical properties in inland waters (Palmer et al., 2015).

The Amazon River receives waters from large and small rivers and exchanges organic and inorganic constituents with floodplains areas that stays under water during months, playing an important role in the biogeochemical processes that occurs in the entire watershed (Richey et al., 1990; Ward et al., 2015). The Lower Amazon is a region that gathers the water received from all the largest Amazon tributary rivers and despite its importance, remote sensing studies in this area are relatively sparse.

In addition to allowing a synoptic monitoring, retrieving CDOM by remote sensing also subsidizes studies that explore the relationship of CDOM with the dissolved organic carbon (DOC) as emphasized by numerous recent studies (Brezonik et al., 2015; Kutser et al., 2015; Vantrepotte et al., 2015) as well as with  $pCO_2$  (Clark et al., 2004, Kutser et al., 2015). Such potential offers new possibilities for increasing our current knowledge on the role of the Amazon River in the global carbon cycle. In this context, the aim of the current study is to explore the performance of current CDOM empirical inversion algorithms for retrieving CDOM in the Lower Amazon River.

## 2. Material and Methods

The study area comprises the Lower Amazon River, a transect of 900 km between the upstream boundary at Óbidos (S 01°55.141', W 55°31.543') and the Amazon River mouth. The downstream boundary was the north and south channel near Macapá, which are the last two well-constrained channels near the Amazon River mouth (S 00°05.400', W 51°03.200' and S 00°09.415', W 50°37.353', respectively). In addition to the Amazon River, samples were also collected in the Tapajos, Xingu, Paru and Jari River as well as at in the Great Lake

Curuai (Figure 1a). These latter rivers are classified as clear waters and generally show high levels of in situ primary production when compared to the turbid Amazon River waters (Ward et al., 2015). The sampling was done during four different seasons: high water (T1, May 2014), low water (T2, November 2014), falling water (T3, July 2015) and rising water (T4, February 2016) (Figure 1).

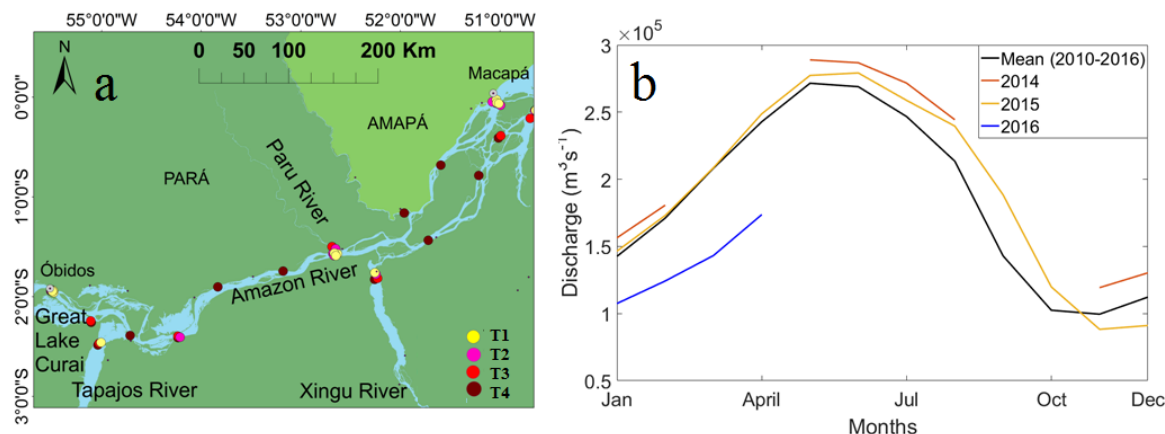


Figure 1. a) In situ sampling stations at the Lower Amazon River and tributaries (Tapajos, Xingu and Paru River); b) Seasonal discharge of the Amazon River during the years of 2014, 2015, 2016, and the mean value during 2010-2016. Discharge data acquired from Óbidos Station (ANA – Brazil’s National Waters Agency).

Water samples were prior filtered through 25 mm Whatman GF/F glass fiber filters (0.7  $\mu\text{m}$  nominal pore size) to remove the suspended matter and the resultant water was refiltered through 0.2  $\mu\text{m}$  polycarbonate membranes (Whatman Nuclepore, 25 mm) under gentle vacuum ( $< 5 \text{ mm Hg}$ ) according to the NASA protocol (Mitchell et al., 2003). Samples were storage in pre-combusted glass bottle wrapped with aluminum foil and kept under refrigeration ( $4^\circ\text{C}$ ) until laboratory analysis. CDOM samples were taken from the refrigerator before starting the analysis with the purpose of regulate it with the room temperature and to avoid any bias due to thermal difference between the samples and the reference water (Milli-Q water). CDOM absorbance spectra were measured from 250 to 850 nm using a Shimadzu, UV 2450 spectrophotometer with a 10cm quartz cell. CDOM absorption coefficient ( $a_{cdom}(\lambda)$ ) are calculated from absorbance measurements using the following Equation 1:

$$a_{cdom}(\lambda) = 2.303 \cdot A(\lambda) / L \quad (1)$$

where  $A(\lambda)$  is the absorbance of the filtered water sample at the specific wavelength  $\lambda$  and  $L$  is the optical pathway of the quartz cell in meters. As recommended by Babin et al. (2003) for waters with higher concentration of CDOM, a baseline correction was applied to each spectrum by subtracting the average absorbance in the range of 680-690 nm to the whole spectrum.

Concurrent to the water sampling, above water radiometry was measured with a portable hyperspectral radiometer FieldSpec® (ASD Inc.). The acquisition geometry followed Mobley (1999) recommendations. Total water leaving radiance ( $L_w$ ), sky radiance ( $L_{sky}$ ) and the radiance from a white panel Spectralon reference ( $L_g$ ) were consecutively measured 6 to 10 times. The later parameter was used to estimate the downwelling irradiance ( $E_d$ ) (Equation 2):

$$E_d(\lambda) = L_g(\lambda) f_c \pi \quad (2)$$

where  $f_c$  is a correction factor estimated in laboratory by the ratio of a standard Spectralon reference that remains in the laboratory by the Spectralon panel used in the field.

The remote sensing reflectance ( $R_{rs}$ ) can be computed according to Equation 3:

$$R_{rs} = \frac{L_w}{E_d} = \frac{L_u - \rho_{air-river} * L_{sky}}{E_d} \quad (3)$$

where  $L_u$  is the upwelling radiance that reaches the sensor and  $\rho_{air-river}$  is a sky glint correction coefficient at the air-sea interface.

There are several methods in the literature to correct the sun glint interference. In the present study we used the approach of Ruddick et al. (2006), here called R06 which is indicated for turbid to highly turbid waters. Its  $\rho_{air-river}$  is a function of wind and cloud cover. It also proposes a correction for residual glint or white offset correction using the bands of  $R_{rs}(780)$  and  $R_{rs}(720)$ .

The coefficient of variation (CV) (Equation 4) of the  $R_{rs}$  spectra replicates was computed for each station. Only the spectrum with CV close or lower than 10% between the interval of 400-840 was kept and the average was calculated to get the final spectrum utilized in this study as representative of  $R_{rs}$  at each station.

$$cv = \frac{\sigma}{\mu} \quad (4)$$

Several empirical algorithms have been developed to estimate CDOM considering various levels of water turbidity and remote sensing sensors. While the blue/green band ratio is often considered as the input parameter of such empirical formulations (Tassan, 1994; Kutser et al., 2005; Mannino et al., 2014), many algorithms have been documented considering alternative band ratios including green/blue (Griffin et al., 2011), green/red (Kutser et al., 2005; Kutser et al., 2015), blue/red (Mannino et al., 2014), red/blue (Tiwari and Shanmugam, 2011) and blue/NIR (Brezonik et al., 2005). Six  $a_{cdom}(412)$  empirical inversion algorithms based on different hypotheses regarding the input parameters have been considered in the frame of this study (Table 1).

Table 1. Empirical algorithms used to retrieve CDOM absorption coefficient in the Lower Amazon River from *in situ*-measured remote sensing reflectance data.

Algorithm	Input Rrs (nm)	Data sets/ study sites	Reference
G11	$\frac{560}{485}$	Kolyma River, East Syberia	Griffin et al., 2011
K05	$\frac{480}{560}$	Lakes in Sweden and Finland	Kutser et al., 2005
B05	$\frac{478}{835}$	Minnesota Lakes, U.S.	Brezonik et al., 2005
M14	$\frac{412}{670}$	Continental margin of the northeastern of U.S.	Mannino et al., 2014
T11	$\frac{670}{490}$	NOMAD dataset, coastal and ocean waters	Tiwari and Shanmugam, 2011
K15	$\frac{559}{664}$	Swedish Lakes	Kutser et al., 2015

### 3. Results and Discussion

The measured CDOM absorption coefficients at the Lower Amazon region presented high values for all stations (N=54). It should be noted that CDOM absorption still present very high values in the green wavelength (i.e.  $a_{CDOM}(560) = \sim 0.4 \text{ m}^{-1}$ ) (Figure 2) and should therefore significantly impact the  $R_{rs}$  spectra in this spectral range.

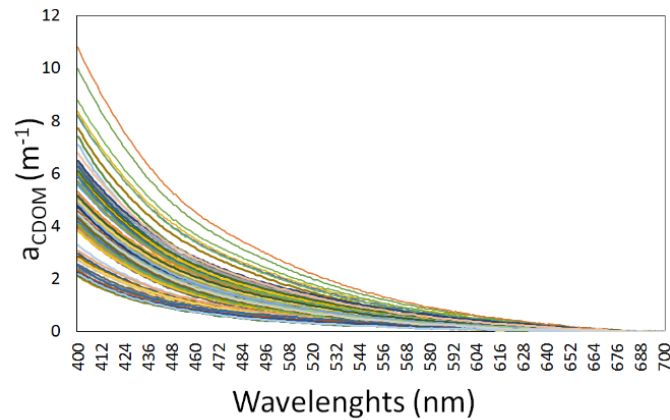


Figure 2. *In situ*-measured CDOM absorption coefficients in all stations at the Lower Amazon River region (N=54).

Although the R06 method shows a good performance with low CV in all spectra, it should be noted that a scatter in the  $R_{rs}$  measurements is still relatively important at 412 nm and 835 nm (Figure 3).

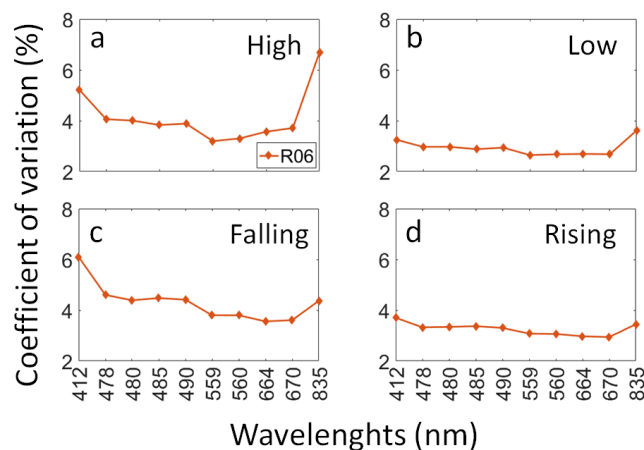


Figure 3. Average of the coefficient of variation (%) for all stations per season sampling. The X axis shows the selected wavelengths for the development of empirical algorithms to estimate CDOM absorption coefficient by remote sensing.

A performance comparison exercise of the six empirical algorithms reported in Table 1, and fitted to our dataset was conducted (Figure 4). Globally, methods based on blue to green ratios (G11 and K05) showed lower performances. This behavior might be caused by the remaining high CDOM absorption in the green part of the spectra (Figure 2) or due to the presence of particulate matter. The approach based on the NIR information (B05) showed also relatively poor potential probably due to the higher uncertainties in our  $R_{rs}$  data in this spectral domain (Figure 3). The M14 and T11 formulations based on the blue and red bands conversely presented a better potential for application in our study region. The relatively lower performance of the M14 algorithm when compared to T11 might be related to the

higher uncertainties in  $R_{rs}$  measurements at 412 nm. The best algorithm performance for our dataset was obtained with the K15 (559/664 nm). This might be due to the fact that the Lower Amazon is a region with high CDOM loads, which still highly influence  $R_{rs}$  values in the green band (Figure 2). It should be noted that the CV of  $R_{rs}$  data in the two bands considered by the latter algorithm are relatively low, explaining the lower scatter in the relationship when compared to other formulations.

Considering the data presented in this study, the relationship between K15 and  $a_{cdom}(412)$  at the Lower Amazon can be describe as follows (Equation 5):

$$a_{CDOM}(412) = 10^{(-0.53.(K15) + 1.05)} \quad (5)$$

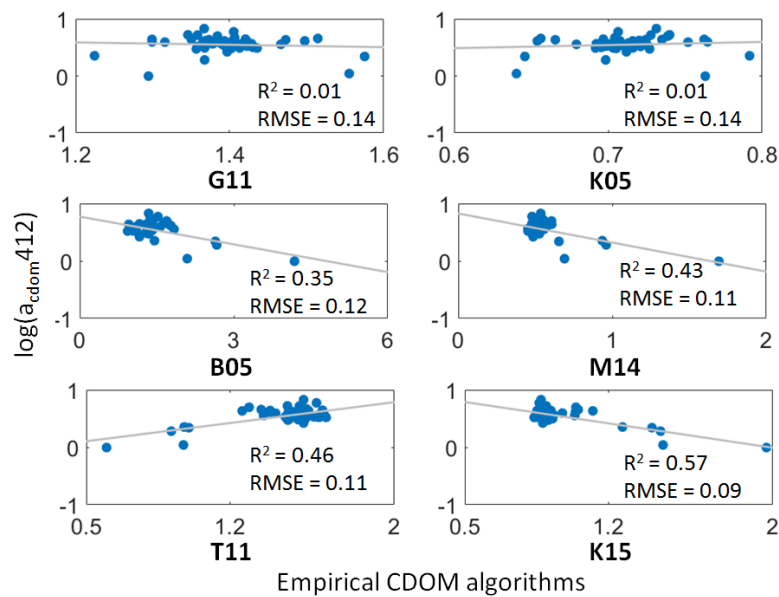


Figure 4. Empirical algorithms used to estimate  $a_{cdom}(412)$  at the Lower Amazon region (see text for bands used in each algorithm).

To better understand the dispersion of the samples around the relationships between  $R_{rs}$  and  $a_{cdom}(412)$ , the dataset was partitioned according to the water color, i.e. splitting Amazon River water and the other rivers (Tapajós, Xingu, Paru and Jari) (Figure 5a), as well as according to the season of data acquisition (Figure 5b). The Amazon River samples are characterized by higher  $a_{cdom}(412)$  values while clear water samples are more scattered, explaining the obtained relationship. Likewise, the season is determinant in the dispersion of the samples, which refers to the mixture of the Amazon waters with the clear waters in the location of sampling. During the Rising and High season, the Amazon River overflows and mixes with other rivers. The K15 algorithm applied to our dataset tends to globally underestimate  $a_{cdom}(412)$  (Bias = -8) with a relative error (Mean Relative Absolute Difference - MRAD) of 15% (Figure 5c).

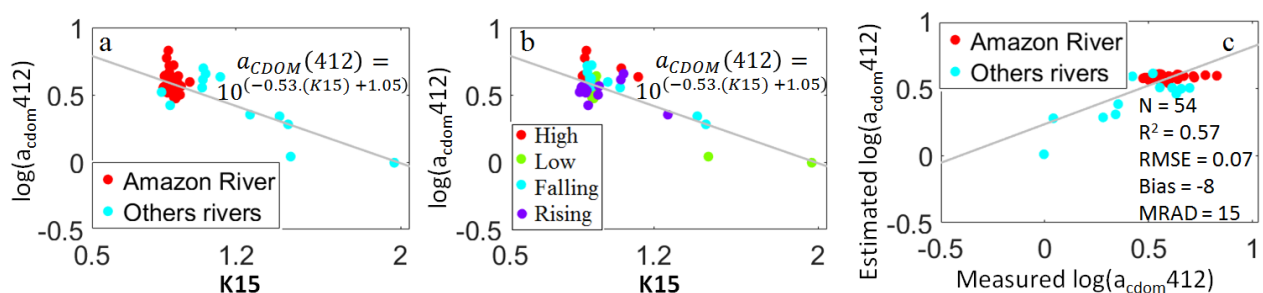


Figure 5. Relationship between  $a_{\text{cdom}}(412)$  and K15 for: a) Amazon River and other rivers (Tapajós, Xingu, Paru and Jari); b) During different sampling season (Rising, High, Falling and Low); c) Plot of measured and estimated  $\log(a_{\text{cdom}}412)$ .

When all the six empirical algorithms are applied to the partitioned samples (Amazon River and others rivers) the results are different (Table 2). It is evident that the clear water river drives the response of the obtained fit when all the samples are considered together. The K15 has no significant relationship when just Amazon samples are considered ( $R^2=0$ ; RMSE = 0.08; p-value>0.05) while its coefficient of determination is higher ( $R^2=0.68$ ; RMSE = 0.14; p-value<0.05) when just the clear water rivers are considered. These results suggest that no simple unique relationship of any band ratio can be used to retrieve  $a_{\text{cdom}}$  from the Amazon River. Otherwise, different approaches should be further explored. It is likely that the poor performance of the band ratio approach presented here is related to the influence of suspended sediments in the water (Brezonik et al., 2015). Considering another spectral band to correct for the influence of the particles could improve the relationship. The optical heterogeneity should be considered when developing a CDOM inversion algorithm retrieval for the Amazonian river waters.

Table 2. Statistics of the relationships between six empirical algorithms and *in situ*-measured  $a_{\text{cdom}}(412)$  when samples are partitioned into Amazon River and Other Rivers groups.

	Amazon River			Other Rivers		
	$R^2$	RMSE	p-value	$R^2$	RMSE	p-value
G11	0,08	0,08	>0,05	0,04	0,24	>0,05
K05	0,12	0,07	<0,05	0,04	0,24	>0,05
B05	0,14	0,07	<0,05	0,44	0,18	<0,05
M14	0,12	0,07	<0,05	0,52	0,17	<0,05
T11	0,01	0,08	>0,05	0,57	0,16	<0,05
K15	0,00	0,08	>0,05	0,68	0,14	<0,05

#### 4. Conclusion

Among all the six empirical algorithms tested in this work, the K15 (559/664 nm) shows the best relationship with  $a_{\text{cdom}}(412)$  when all samples are considered. When the samples are partitioned into Amazon River and Other Rivers (clear water rivers) the relationships are different. All the empirical algorithms presented a higher coefficient of determination when just clear water rivers are considered, and no significant relationship is obtained when just the Amazon River is considered. The results suggest that other optically active constituent might be interfering in the CDOM retrieval and it is likely to be suspended sediments. Therefore, different approaches should be explored to correct for the influence of particles, such as, for instance, adding another spectral band or developing a specific index for suspended sediments. The difference observed between the relationship of the inversion algorithm for the Amazon River and for the clear water rivers also foments the discussion about the necessity of having two different algorithms, specific for each water type or a more general algorithm that is independent of this variability. It is also shown that the sampling season is also determinant in the algorithm performance for  $a_{\text{cdom}}(412)$  estimation. During the Rising and High season, the Amazon water is mixed with clear waters enhancing its CDOM loads. Our results are a step forward to the understanding of the relationship between  $R_{\tau_S}$  and  $a_{\text{cdom}}(412)$  in the Lower

Amazon region and contributes with remote sensing application in the study of very turbid inland waters.

## References

- Babin, M.; Stramski, D.; Ferrari, G. M.; Claustre, H.; Bricaud, A.; Obolensky, G.; Hoepffner, N. Variations in the light absorption coefficients of phytoplankton, nonalgal particles, and dissolved organic matter in coastal waters around Europe. **Journal of Geophysical Research**, v. 108, n. C7, p. 3211, 2003.
- Brezonik, P. L.; Olmanson, L. G.; Finlay, J. C.; Bauer, M. E. Factors affecting the measurement of CDOM by remote sensing of optically complex inland waters. **Remote Sensing of Environment**, v. 157, p. 199–215, 2015.
- Brezonik, P.; Menken, K. D.; Bauer, M. Landsat-based remote Sensing of Lake Water Quality Characteristics, Including Chlorophyll and Colored Dissolved Organic Matter (CDOM). **Lake and Reservoir Management**, v. 21, n. 4, p. 373–382, 2005.
- Clark, C. D.; Hiscock, W. T.; Millero, F. J.; Hitchcock, G.; Brand, L.; Miller, W. L.; Ziolkowski, L.; Chen, R. F.; Zika, R. G. CDOM distribution and CO<sub>2</sub> production on the Southwest Florida Shelf. **Marine Chemistry**, v. 89, n. 1–4, p. 145–167, 2004.
- Griffin, C. G.; Frey, K. E.; Rogan, J.; Holmes, R. M. Spatial and interannual variability of dissolved organic matter in the Kolyma River, East Siberia, observed using satellite imagery. **Journal of Geophysical Research: Biogeosciences**, v. 116, n. 3, p. 1–12, 2011.
- Kutser, T.; Pierson, D. C.; Kallio, K. Y.; Reinart, A.; Sobek, S. Mapping lake CDOM by satellite remote sensing. **Remote Sensing of Environment**, v. 94, n. 4, p. 535–540, 2005.
- Kutser, T.; Verpoorter, C.; Paavel, B.; Tranvik, L. J. Estimating lake carbon fractions from remote sensing data. **Remote Sensing of Environment, ocean optics**, v. 157, p. 138–146, 2015.
- Mannino, A.; Novak, M. G.; Hooker, S. B.; Hyde, K.; Aurin, D. Algorithm development and validation of CDOM properties for estuarine and continental shelf waters along the northeastern U.S. coast. **Remote Sensing of Environment**, v. 152, p. 576–602, 2014.
- Mitchell, B.G.; Kahru M.; Wieland J.; Stramska M. Determination of spectral absorption coefficients of particles, dissolved material and phytoplankton for discrete water samples, in: **Ocean Optics Protocols for Satellite Ocean Color Sensor Validation**, J. L. Mueller, G. D. Fargion and C. R. McClain, eds. (NASA Goddard Space Flight Center, 2003).
- Mobley, C. D. Estimation of the remote-sensing reflectance from above-surface measurements. **Applied optics**, v. 38, n. 36, p. 7442–55, 1999.
- Palmer, S. C. J.; Kutser, T.; Hunter, P. D. Remote sensing of inland waters : Challenges, progress and future directions. **Remote Sensing of Environment**, v. 157, p. 1–8, 2015.
- Richey, J. E.; Hedges, J. I.; Devol, A. H.; Quay, P. D.; Victoria, R.; Martinelli, L.; Forsberg, B. R. Biogeochemistry of carbon in the Amazon River. **Limnology and Oceanography**, v. 35, n. 2, p. 352–371, 1990.
- Ruddick, K. G.; Cauwer, V. DE; Park, Y.; Moore, G. Seaborne measurements of near infrared water-leaving reflectance : The similarity spectrum for turbid waters. **Limnol. Oceanogr.**, v. 51, n. 2, p. 1167–1179, 2006.
- Tassan, S. Local algorithms using SeaWiFS data for the retrieval of phytoplankton, pigments, suspended sediment, and yellow substance in coastal waters. **Applied optics**, v. 33, n. 12, p. 2369–78, 1994.
- Tiwari, S. P.; Shanmugam, P. An optical model for the remote sensing of coloured dissolved organic matter in coastal/ocean waters. **Estuarine, Coastal and Shelf Science**, v. 93, n. 4, p. 396–402, 2011.
- Vantrepotte, V.; Danhiez, F.; Loisel, H.; Mériaux, X.; Cauvin, A.; Dessailly, D. CDOM-DOC relationship in contrasted coastal waters : implication for DOC retrieval from ocean color remote sensing observation. **Optics Express**, v. 23, n. 1, p. 578–590, 2015.
- Ward, N. D.; Krusche, A. V.; Sawakuchi, H. O.; Brito, D. C.; Cunha, A. C.; Moura, J. M. S.; Da Silva, R.; Yager, P. L.; Keil, R. G.; Richey, J. E. The compositional evolution of dissolved and particulate organic matter along the lower Amazon River-Obidos to the ocean. **Marine Chemistry**, v. 177, p. 244–256, 2015.
- Wetzel, R. G.; Likens, G. E. **Limnological Analyses**. 3. ed., 2000.
- Zhu, W.; Yu, Q.; Tian, Y. Q.; Becker, B. L.; Zheng, T.; Carrick, H. J. An assessment of remote sensing algorithms for colored dissolved organic matter in complex freshwater environments. **Remote Sensing of Environment**, v. 140, p. 766–778, 2014.